EPJ Web of Conferences **126**, 04030 (2016) DOI: 10.1051/epjconf/201612604030
ICNFP 2015

Recent observation of D^{**} and D_s^{**} at Belle

Dmitry Matvienko[1,a]
on behalf of the Belle Collaboration

[1] *Budker Insitute of Nuclear Physics, SB RAS, Novosibirsk, 630090 and Novosibirsk State University, Novosibirsk, 630090*

Abstract. We report on the first observation of $\bar{B}^0 \to D_1(2430)^0\omega$, $\bar{B}^0 \to D_1(2420)^0\omega$ and $\bar{B}^0 \to D_2^*(2460)^0\omega$ decays and determination of their rates as well as the fractions of longitudinal polarizations of the ω for these decays. We also discuss improved measurements of the $B \to DD_{s0}^*(2317)$ branching fractions with a search for isospin partners of the $D_{s0}^*(2317)^+$ state, $\mathbf{z}^0$ and $\mathbf{z}^{++}$. These measurements use a data sample containing 772 million $B\bar{B}$ events collected at the $\Upsilon(4S)$ resonance with the Belle detector at the KEKB asymmetric-energy e^+e^- collider.

1 Introduction

Since 2004, significant success in observation of orbitally and radially excited heavy-light mesons has been achieved in several experiments, such as Belle [1], *BABAR* [2], LHCb [3] etc.

The relativistic quark model [4] predicts four physical states with a P-wave orbital excitation in the charm and charm-strange meson families. They have spin-parities $J^P = 0^+$ ($j = 1/2$), 1^+ ($j = 1/2$), 1^+ ($j = 3/2$) and 2^+ ($j = 3/2$), where $j = s \pm 1$ and s is the spin of the light quark in the meson. The states with $j = 1/2$ are expected to be broad (hundreds of MeV/c^2), while the states with $j = 3/2$ are expected to be narrow (tens of MeV/c^2 or smaller). All these states have been discovered [5]. They are $D_0^*(2400)$, $D_1(2430)$, $D_1(2420)$ and $D_2^*(2460)$ (D^{**} states) in the charm sector as well as $D_{s0}^*(2317)$, $D_{s1}(2460)$, $D_{s1}(2536)$ and $D_{s2}(2573)$ (D_s^{**} states) in the charm-strange sector. The observed masses and widths for the D^{**} states are in reasonable agreement with the quark model predictions. However, this is not the case for the D_s^{**} states. The conventional $c\bar{s}$ hypothesis contradicts to experimentally measured masses, widths and relative branching fractions of the P-wave excitations of the D_s meson.

Here, we discuss two recent Belle measurements of the neutral B decays to the $D^{**}\omega$ final state [6], where D^{**} states are reconstructed in the $D^*\pi$ mode, and the neutral and charged B decays to the $\bar{D}D_{s0}^{*+}(2317)$ final state [7]. The Belle detector [8] at the KEKB asymmetric-energy e^+e^- (3.5 on 8 GeV) collider [9] is used to study B mesons produced in the reaction $e^+e^- \to \Upsilon(4S) \to B\bar{B}$. The $B\bar{B}$ integrated luminosity of 711 fb^{-1} contains $(772 \pm 11) \times 10^6$ $B\bar{B}$ pairs. The studies presented here, $\bar{B}^0 \to D^{**}\omega$ and $B \to \bar{D}D_{s0}^{*+}(2317)$, use the complete Belle data set.

[a] e-mail: d.v.matvienko@inp.nsk.su

2 D^{**} production in semileptonic and hadronic B decays

Study of D^{**} production in semileptonic B decays is of interest for several reasons. Firstly, $\bar{B} \to D^{**} l^- \bar{\nu}_l$ decays constitute a significant fraction of B semileptonic decays and may help to explain the origin of the $\sim 3\sigma$ discrepancy between exclusive and inclusive determinations of the Cabibbo-Kobayashi-Maskawa matrix element $|V_{\rm cb}|$. It is therefore interesting to learn more about the composition of the final hadronic state X_c in the inclusive $\bar{B} \to X_c l^- \bar{\nu}_l$ decay. Moreover, the measured decay properties for $\bar{B} \to D^{**} l^- \bar{\nu}_l$ can be compared with QCD sum rules [10] and predictions from heavy quark effective theory (HQET) [11]. It has been found that these properties for narrow $j = 1/2$ D^{**} states are in serious conflict with the theoretical expectations. Semileptonic B decay rates to the D^{**} states depending on the invariant four-velocity transfer w are estimated as:

$$\frac{d\Gamma(B \to D^{**}_{j=1/2} l\nu)}{dw} \propto G_F^2 |V_{\rm cb}|^2 K_{1/2}(w) |\tau_{1/2}(w)|^2,$$
$$\frac{d\Gamma(B \to D^{**}_{j=3/2} l\nu)}{dw} \propto G_F^2 |V_{\rm cb}|^2 K_{3/2}(w) |\tau_{3/2}(w)|^2,$$

where K_j are known kinematical factors with hierarchy of $K_{1/2}(w) < K_{3/2}(w)$, and $\tau_j(w)$ are Isgur-Wise functions with predicted $\tau_{1/2}(w) << \tau_{3/2}(w)$ behavior [11]. Thus, HQET and QCD sum rules predict the suppression of $j = 1/2$ states relative to the $j = 3/2$. However, experimental measurements demonstrate comparable rates for $j = 1/2$ and $j = 3/2$. Herewith, the observed rates for $j = 3/2$ states are in good agreement with predictions. This is a so called "1/2 semileptonic puzzle". There are different attempts to solve this problem [12, 13] but, at this moment, the full understanding is absent. To elucidate this problem, it is useful to study non-leptonic B decays to D^{**}.

Non-leptonic B decays to D^{**} states and a light hadronic system (to be specific we will discuss a pion here) can be divided into three classes. Class I $\bar{B}^0 \to D^{**+}\pi^-$ decays describe the color-favored pion emission process, class II $\bar{B}^0 \to D^{**0}\pi^0$ decays correspond to the color-suppressed D^{**} emission process and class III $B^- \to D^{**0}\pi^-$ decays comprise these two emission processes. Experimental results for non-leptonic relative decay rates are shown in Table 1 for class I and class III decays. Class II $\bar{B}^0 \to D^{**0}\pi^0$ decays have not been observed so far. All entries corresponding to the class

Table 1. Observed branching fraction (BF) products for $B \to D^{**}\pi$ class I and class III decays.

Class	BF product	Value
Class I	$\mathcal{B}(\bar{B}^0 \to D_0^*(2400)^+\pi^-) \times \mathcal{B}(D_0^*(2400)^+ \to D^0\pi^+)$	$(6.0 \pm 3.0) \times 10^{-5}$
	$\mathcal{B}(\bar{B}^0 \to D_1(2430)^+\pi^-) \times \mathcal{B}(D_1(2430)^+ \to D^{*0}\pi^+)$	$< 7 \times 10^{-5}$
	$\mathcal{B}(\bar{B}^0 \to D_1(2420)^+\pi^-) \times \mathcal{B}(D_1(2420)^+ \to D^{*0}\pi^+)$	$(3.7 \pm 0.9) \times 10^{-4}$
	$\mathcal{B}(\bar{B}^0 \to D_2^*(2460)^+\pi^-) \times \mathcal{B}(D_2^*(2460)^+ \to D^0\pi^+)$	$(2.2 \pm 0.4) \times 10^{-4}$
	$\mathcal{B}(\bar{B}^0 \to D_2^*(2460)^+\pi^-) \times \mathcal{B}(D_2^*(2460)^+ \to D^{*0}\pi^+)$	$(2.5 \pm 0.6) \times 10^{-4}$
Class III	$\mathcal{B}(\bar{B}^- \to D_0^*(2400)^0\pi^-) \times \mathcal{B}(D_0^*(2400)^0 \to D^-\pi^+)$	$(6.4 \pm 1.4) \times 10^{-4}$
	$\mathcal{B}(\bar{B}^- \to D_1(2430)^0\pi^-) \times \mathcal{B}(D_1(2430)^0 \to D^{*-}\pi^+)$	$(5.0 \pm 1.3) \times 10^{-4}$
	$\mathcal{B}(\bar{B}^- \to D_1(2420)^0\pi^-) \times \mathcal{B}(D_1(2420)^0 \to D^{*-}\pi^+)$	$(6.8 \pm 1.5) \times 10^{-4}$
	$\mathcal{B}(\bar{B}^- \to D_2^*(2460)^0\pi^-) \times \mathcal{B}(D_2^*(2460)^0 \to D^-\pi^+)$	$(3.5 \pm 0.4) \times 10^{-4}$
	$\mathcal{B}(\bar{B}^- \to D_2^*(2460)^0\pi^-) \times \mathcal{B}(D_2^*(2460)^0 \to D^{*-}\pi^+)$	$(2.2 \pm 1.1) \times 10^{-4}$

III decays in Table 1 are of the same order, whereas class I decays to the broad $j = 1/2$ states are one order of magnitude smaller than decays to the narrow $j = 3/2$ states. Moreover, class I and class III decays to the $j = 3/2$ states are similar in size. This hierarchy of the decay rates is theoretically

understood. Using the factorisation and predictions for $\tau_j(w)$ functions in heavy quark limit together with finite corrections to HQET one obtains striking agreement between theory and experiment for class I decays. Class III results can be also explained because there is an extra D^{**} emission diagram here, which is expected to be suppressed for $j = 3/2$ states, but not for $j = 1/2$ due to heavy quark symmetry (HQS). However, there are no observed class II decays with the D^{**} emission process only. Therefore, it is interesting to confirm this prediction from experimental measurements. The recent Belle study of the $\bar{B}^0 \to D^{**0}\omega$ decays solves this problem.

2.1 $B \to D^{**}\omega$ analysis strategy

Observation of the class II hadronic decays allows one to answer the following questions: what are the $j = 1/2$ and $j = 3/2$ rates in class II decays and what is the tensor rate in these decays? It is obvious that the tensor state $D_2^*(2460)^0$ cannot be generated by the V-A current and should be absent in the factorisation approximation. Moreover, it should be suppressed by HQS. Nevertheless, soft collinear effective theory (SCET) [14] predicts nontrivial production of this state as well as the equality of brancnhing fractions and strong phases in the decays $\bar{B}^0 \to D_2^*(2460)^0 M$ and $\bar{B}^0 \to D_1(2420)^0 M$, where $M = \pi, \rho, K$ or K^* with longitudinal polarization.

We have chosen to analyse class II $\bar{B}^0 \to D^{**0}\omega$ decays for several reasons. Firstly, lower fractions of $q\bar{q}$ continuum and combinatorial backgrounds are expected in this mode relative to the $\bar{B}^0 \to D^{**0}\pi^0$ decays. Further, we can measure the polarisations and partial-wave fractions of the D^{**} states. Finally, we can perform the coherent study of the ρ-meson-like state in the $\omega\pi$ final state.

All B candidates in this analysis are identified using two kinematic variables: the energy difference $\Delta E = \sum_i \sqrt{|\mathbf{p}_i^*|^2 c^2 + m_i^2 c^4} - E^*_{\rm beam}$ and the beam-constrained mass $M_{\rm bc} = \sqrt{E^{*2}_{\rm beam}/c^4 - |\sum_i \mathbf{p}_i^*|^2/c^2}$, where the summation is over all particles forming the B candidate, $\mathbf{p}_i^*$ and m_i are their three-momenta and masses, respectively, and $E^*_{\rm beam}$ is the beam energy. All quantities are defined in the e^+e^- c.m. frame. These variables allow one to select the signal sample with the small background fraction. We use a tight cut on $M_{\rm bc}$ corresponding to about ± 2 times the mass resolution and loose cuts on ΔE and invariant mass $M(\pi^+\pi^-\pi^0)$ of the ω.

Figure 1 shows the distribution of the selected events in the $\Delta E - M(\pi^+\pi^-\pi^0)$ plane, where we define four regions to distinguish between signal and background:the signal region I and sideband regions II, III and IV. The background component in the signal region I is described by the functions, which are determined in the control sideband regions II, III and IV in Fig. 1.

To distinguish the contributions for narrow and broad D^{**} states in the signal region, coherent amplitude analysis is performed. This analysis minimises the likelihood function in the six-dimensional kinematic phase space of the decay. The likelihood function is constructed from the background and signal probability density functions (PDF).

In total, six variables are required to fully describe $D^*\omega\pi$ kinematics. We define two sets of kinematic variables, corresponding to the $\omega\pi$ and D^{**} production. Each of the sets includes the invariant mass squared of the intermediate state ($\omega\pi$ or D^{**}) and five angular variables. The angles describing $\omega\pi$ production are defined in Fig. 2. Similar variables are also defined for the D^{**} contribution. All the D^{**} states are well distinguished by their angular distributions.

The signal PDF is equal to the decay matrix element squared, where a six-dimensional amplitude is written as a sum of the Breit-Wigner factors with angular parts. These factors describe the production and decay of the intermediate resonances, ρ-meson-like and D^{**} states [15]. The model parameters in the matrix element and observables are determined from the unbinned likelihood fit in the signal region.

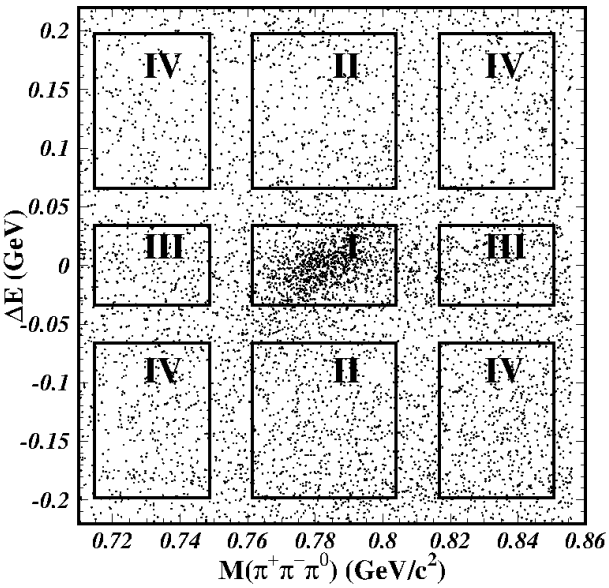

Figure 1. Distribution of ΔE versus $M(\pi^+\pi^-\pi^0)$ for the selected $\bar{B}^0 \to D^{*+}\omega\pi^-$ candidates. The signal region (I) and sideband regions (II, III and IV) are shown.

2.2 D^{**} polarizations and branching fraction products

The distributions of the $D^*\pi$ and $\omega\pi$ invariant masses squared for the $D^{*+}\omega\pi^-$ candidates in the signal $\Delta E - M(\pi^+\pi^-\pi^0)$ region I are shown in Figs. 3 (a) and (b). These distributions correspond to kinematic regions of phase space enriched (Fig. 2 (a)) and depleted (Fig. 2 (b)) with D^{**} mesons. The results of the fit with the considered signal model are superimposed. The plots demonstrate a reasonable description of the data by the fit. The fit results require large signals for the $\rho(770)$ and $\rho(1450)$ contributions with branching fraction products of $(1.48 \pm 0.27\,(\text{stat.})\,^{+0.15}_{-0.09}\,(\text{syst.})\,^{+0.21}_{-0.56}\,(\text{model})) \times 10^{-3}$ and $(1.07\,^{+0.15}_{-0.31}\,(\text{stat.})\,^{+0.06}_{-0.13}\,(\text{syst.})\,^{+0.40}_{-0.02}\,(\text{model})) \times 10^{-3}$, respectively. The combined first-class current branching fraction product $(1.90 \pm 0.11\,(\text{stat.})\,^{+0.11}_{-0.13}\,(\text{syst.})\,^{+0.02}_{-0.06}\,(\text{model})) \times 10^{-3}$ is well measured and has small model uncertainties.

Color-suppressed decays saturated by the $\bar{B}^0 \to D_1(2430)^0\omega$ decays with branching fraction product of $(2.5 \pm 0.4\,(\text{stat.})\,^{+0.7}_{-0.2}\,(\text{syst.})\,^{+0.4}_{-0.1}\,(\text{model})) \times 10^{-4}$ and $\bar{B}^0 \to D_1(2420)^0\omega$ with a significantly smaller branching fraction product of $(0.7 \pm 0.2\,(\text{stat.})\,^{+0.1}_{-0.0}\,(\text{syst.}) \pm 0.1\,(\text{model})) \times 10^{-4}$ are observed in the studied mode. The fit results also require a non-trivial fraction of $(0.4 \pm 0.1\,(\text{stat.})\,^{+0.0}_{-0.1}\,(\text{syst.}) \pm 0.1\,(\text{model})) \times 10^{-4}$ for the non-factorizable $\bar{B}^0 \to D_2(2460)^0\omega$ decay.

The individual partial-wave fractions for D^{**} production have been measured with the comparable probabilities of about 30%. The longitudinal polarizations for D^{**}-production have been also measured. The results, $(63.0 \pm 9.1(\text{stat.}) \pm 4.6(\text{syst.})^{+4.6}_{-3.9}(\text{model.}))\%$ for the $D_1(2430)^0$ production and $(67.1 \pm 11.7(\text{stat.})^{+0.0}_{-4.2}(\text{syst.})^{+2.3}_{-2.8}(\text{model.}))\%$ for the $D_1(2420)^0$ production, have large errors, but imply non-trivial non-factorizable QCD effects in the color-suppressed channel [16].

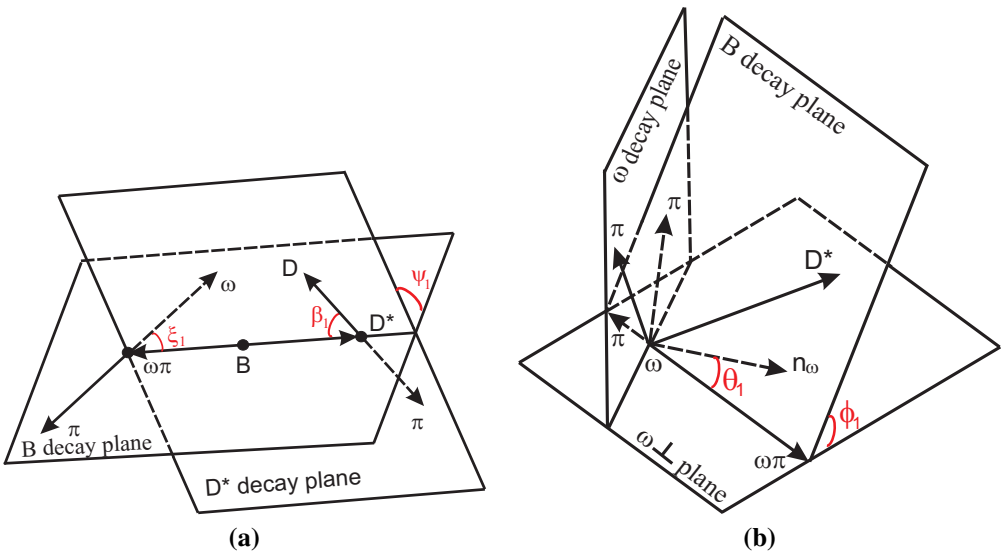

Figure 2. Kinematics of a $\bar{B}^0 \to D^{*+}\omega\pi^-$ decay mediated by an $\omega\pi^-$ intermediate resonance. The diagram in (a) defines two polar angles ξ_1 and β_1 and one azimuthal angle ψ_1. The diagram in (b) defines one polar angle θ_1 and one azimuthal angle ϕ_1. The direction n_ω in (b) corresponds to the vector normal to the ω decay plane.

3 Is the $D^*_{s0}(2317)$ molecule or tetraquark?

The $D^{*+}_{s0}(2317)$ state has been first observed by BaBar [17] and confirmed by CLEO [18] in 2003. Its mass has been measured below the DK threshold despite the potential model prediction based on the $J^P = 0^+$ P-wave $c\bar{s}$ hypothesis. Moreover, CLEO placed a stringent 90% confidence level upper limit on the relative partial width of the radiative $D^{*+}_{s0}(2317) \to D^{*+}_s\gamma$ and strong $D^{*+}_{s0}(2317) \to D^+_\pi\pi^0$ decays, which is 0.059.

The observation of a sub-threshold mass has led to speculations about the nature of its quark bound state. The most popular hypotheses are DK molecule [19] and tetraquark [20] models. Both these models predict the mass of the $D^{*+}_{s0}(2317)$ below the DK threshold. However, they have significantly different estimations of the radiative and strong widths of studied state.

If it is assumed that the $D^{*+}_{s0}(2317)$ is a candidate for DK molecule with isospin quantum number I of $I = 0$, we derive the following estimations for radiative $\Gamma_{\rm rad}$ and strong $\Gamma_{\rm str}$ widths: $\Gamma_{\rm rad} \sim 120$ KeV and $\Gamma_{\rm str} \sim 10$ KeV, where their ratio is near the experimental upper limit. According to heavy quark symmetry, the molecular hypothesis predicts also BK and B^*K molecules. Their radiative decays to $B^{(*)}\gamma$ final states are the best chance for discovery of these states.

It is difficult to satisfy the upper limit of 0.059 in the frame of the tetraquark hypothesis with $I = 0$, while the assignment $I = 1$ changes the situation [20]. In other words, if $D^{*+}_{s0}(2317)$ is assigned to the isotriplet scalar four-quark meson, the CLEO upper limit can be easily satisfied because $\Gamma_{\rm rad} \sim 0.8$ keV and $\Gamma_{\rm str} \sim (4-5)$ MeV in this model. The isotriplet tetraquark model predicts the existence of isospin partners for the $D^{*+}_{s0}(2317)$ state, $\mathbf{z}^0$ and $\mathbf{z}^{++}$. The recent Belle study of the $B^+ \to \bar{D}^0 D^{*+}_{s0}(2317)$ and $B^0 \to D^- D^{*+}_{s0}(2317)$ decays tests this model.

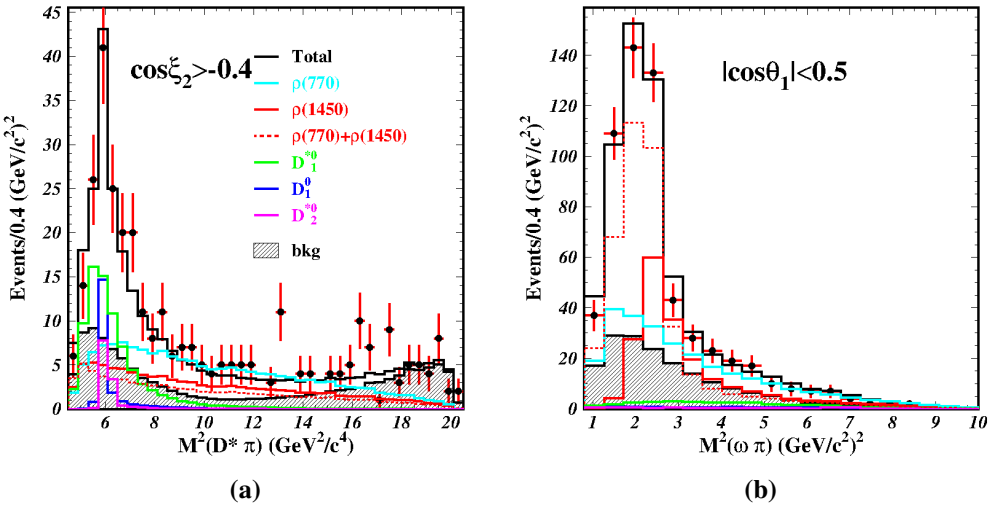

Figure 3. Distributions of the $D^*\pi$ and $\omega\pi$ invariant masses squared for selected $D^{*+}\omega\pi^-$ candidates corresponding to the D^{**} (a) enriched and (b) depleted kinematic regions of phase space.

3.1 Measurement of $B \to \bar{D}D^{*+}_{s0}(2317)$

All B candidates are also identified by the ΔE and $M_{\rm bc}$ variables as in $\bar{B}^0 \to D^{**0}\omega$ decays but with a sufficiently broad window $M_{\rm bc} > 5.20\,{\rm GeV}/c^2$. The $D^{*+}_{s0}(2317)$ candidates are reconstructed in the $D^+_s\pi^0$ mode and D^+_s mesons are identified via their $\pi^+K^+K^-$ decay mode. Candidates for D^- mesons in the neutral B decays are formed via the $K^+\pi^-\pi^-$ decay mode and D^0 mesons in the charged B decays via the $K^-\pi^+$ and $K^+\pi^+\pi^-\pi^-$ decay modes.

We select events in the three-dimensional region of $M_{\rm bc}$, ΔE and invariant mass $M(D^+_s\pi^0)$ variables and perform the unbinned likelihood fit in this space. We form the signal region in these dimensions and use here the signal PDFs in the fit. The outside region is described by the signal and background PDFs in the appropriate variables. The background PDF includes two components to describe combinatorial and peaking backgrounds. The latter peaks in ΔE and $M_{\rm bc}$ (but not $M(D^+_s\pi^0)$) mostly from three-body $B \to \bar{D}\pi^0 D^+_s$ decays. Figure 4 shows the results of the fit for the neutral B decays in the signal regions of the two variables not being plotted. The measured branching fraction product is $\mathcal{B}(B^0 \to D^- D^*_{s0}(2317)^+) \times \mathcal{B}(D^*_{s0}(2317)^+ \to D^+_s\pi^0) = (1.02^{+0.13}_{-0.12} \pm 0.11) \times 10^{-3}$. Similar fit results are obtained for the charged B decays. The measured branching fraction product is $\mathcal{B}(B^+ \to \bar{D}^0 D^*_{s0}(2317)^+) \times \mathcal{B}(D^*_{s0}(2317)^+ \to D^+_s\pi^0) = (0.80^{+0.13}_{-0.12} \pm 0.12) \times 10^{-3}$. All these results agree well with the existing PDG world-average values and significantly improve their precision [5].

3.2 Search for isospin partners of the $D^{*+}_{s0}(2317)$

The isospin partners of the $D^{*+}_{s0}(2317)$, $\mathbf{z}^0$ and $\mathbf{z}^{++}$, have been searched for in the $B^0 \to \bar{D}^0 D^+_s\pi^-$ and $B^+ \to D^- D^+_s\pi^+$ decay channels. Since the $\mathbf{z}^0$ and $\mathbf{z}^{++}$ are hypothetical, their masses are expected to lie within a $\pm 10\,{\rm MeV}/c^2$ mass region of the $D^{*+}_{s0}(2317)$ mass. To be certain that we cover the whole reasonable mass region, we scan for $\mathbf{z}^0$ and $\mathbf{z}^{++}$ signals in 13 adjacent mass bins, covering a ± 32.5 interval around the measured $D^{*+}_{s0}(2317)$ mass, which is 2317.8 MeV.

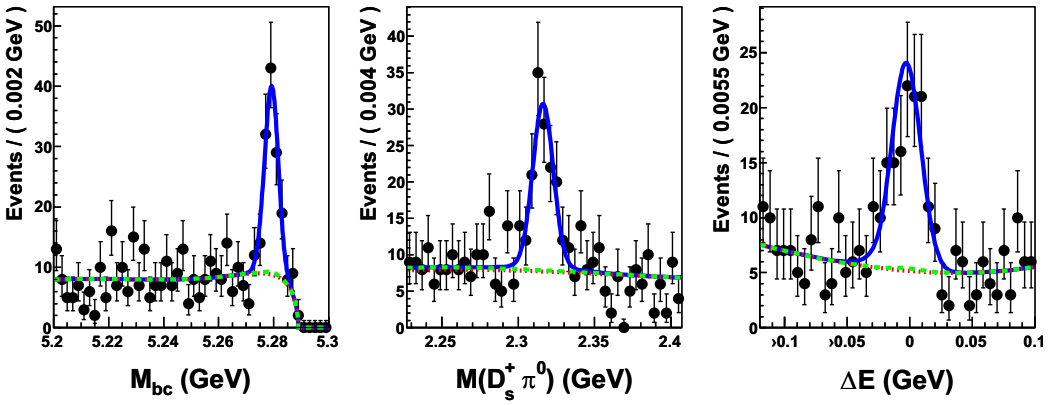

Figure 4. The $M_{\rm bc}$ (left), $M(D_s^+\pi^0)$ (center) and ΔE (right) distributions for projections of the $B^0 \to D^- D_{s0}^{*+}$ candidates that are in the signal regions of the two variables are not being plotted. The red short-dashed curve is the fitted background; the green long-dashed curve describes the peaking background and the solid blue curve includes the signal.

A three-dimensional fit to the data, similar to the measurement of $B \to \bar{D} D_{s0}^{*+}(2317)$, is performed in each studied mass bin. The possible peaking backgrounds are studied using a Monte Carlo sample of generic B meson decays without $\mathbf{z}^0$ and $\mathbf{z}^{++}$ signals. None of the fits returns a positive $\mathbf{z}^0$ or $\mathbf{z}^{++}$ signal with a statistical significance of more than 1.3σ. Assuming the masses of the $\mathbf{z}^0$ and $\mathbf{z}^{++}$ are the same as the $D_{s0}^{*+}(2317)$ we obtain the following 90% confidence level upper limits on the product branching fractions: $\mathcal{B}(B^0 \to \bar{D}^0 \mathbf{z}^0) \times \mathcal{B}(\mathbf{z}^0 \to D_s^+ \pi^-) < 0.64 \times 10^{-4}$ and $\mathcal{B}(B^+ \to D^- \mathbf{z}^{++}) \times \mathcal{B}(\mathbf{z}^{++} \to D_s^+ \pi^+) < 0.27 \times 10^{-4}$. The upper limits on the product branching fractions in other mass bins are close to the values obtained in the central bin. All these upper limits are significantly smaller than the tetraquark predictions with $I = 1$.

4 Conclusion

The recent Belle measurement of $\bar{B}^0 \to D^{*+}\omega\pi^-$ showed the relative dominance of the broad $D_1(2430)^0$ production relative to the narrow $D_1(2420)^0$ in agreement with HQET studies. The significant $\bar{B}^0 \to D_2(2460)^0\omega$ decay has been also observed. Multidimensional coherent amplitude analysis allows one to measure non-factorizable D^{**} polarisations and their partial-wave rates. Moreover, it allows one to perform the first consistent study of the $\rho(770)$ and $\rho(1450)$ states in B meson decays.

New Belle measurements of $B \to \bar{D} D_{s0}^{*+}(2317)$ decays are consistent with the previous experimental results but they have higher precision. The upper limits for the $\mathbf{z}^0$ and $\mathbf{z}^{++}$ decay rates have been obtained. The results are more than one magnitude smaller than the $D_{s0}^{*+}(2317)$-tetraquark predictions with isospin $I = 1$.

Acknowledgements

This work is supported by the Ministry of Education and Science of the Russian Federation and the Russian Foundation for Basic Research under Grant No. 14-02-31527.

References

[1] K. Abe *et al.* (Belle Collaboration), Phys. Rev. D **69**, 112002 (2004); A. Kuzmin *et al.* (Belle Collaboration), Phys. Rev. D **76**, 012006 (2007); D. Liventsev *et al.* (Belle Collaboration), Phys. Rev. D **77**, 091503 (2008).

[2] B. Aubert *et al.* (BaBar Collaboration), Phys. Rev. Lett. **101**, 261802 (2008); B. Aubert *et al.* (BaBar Collaboration), Phys. Rev. D **79**, 112004 (2009).

[3] R. Aaji *et al.* (LHCb Collaboration), Phys. Rev. D **87**, 092001 (2013); R. Aaji *et al.* (LHCb Collaboration), Phys. Rev. D **92**, 032002 (2015).

[4] S. Godfrey and K. Moats, arXiv:1510.08305 and references therein.

[5] K.A. Olive *et al.* (Particle Data Group), Chin. Phys. C **38**, 090001 (2014).

[6] D. Matvienko *et al.* (Belle Collaboration), Phys. Rev. D **92**, 012013 (2015).

[7] S.-K. Choi *et al.* (Belle Collaboration), Phys. Rev. D **91**, 092011 (2015).

[8] A. Abashian *et al.* (Belle Collaboration), Nucl. Instrum Methods Phys. Res., Sect. A **479**, 117 (2002); also see detector section in J. Brodzicka *et al.*, Prog. Theor. Exp. Phys. **2012**, 04D001 (2012).

[9] S. Kurokawa and E. Kikutani, Nucl. Instrum. Methods Phys. Res., Sect. A **499**, 1 (2003), and other papers included in this volume; T. Abe *et al.*, Prog. Theor. Exp. Phys. **2013**, 03A001 (2013) and following articles up to 03A011.

[10] N. Uraltsev, Phys. Lett. B **501**, 86 (2001).

[11] M. Neubert, Phys. Rep. **245**, 259 (1994).

[12] R. Clein, T. Mannel, F. Shahriaran and D. van Dyk, Phys. Rev. D **91**, 094034 (2015).

[13] B. Blossier, arXiv:1411.3563.

[14] S. Mantry, Phys. Rev. D **70**, 114006 (2004).

[15] D.V. Matvienko, A.S. Kuzmin, and S.I Eidelman, J. High Energy Phys. 09 (2011) 129.

[16] H.Y. Cheng, C.K. Chua, and A. Soni, Phys. Rev. D **71**, 014030 (2005).

[17] B. Aubert *et al.* (BaBar Collaboration), Phys. Rev. Lett. **90**, 242001 (2003).

[18] D. Besson *et al.* (CLEO Collaboration), Phys. Rev. D **68**, 032002 (2003).

[19] T. Barnes, F.E. Close and H.J. Lipkin, Phys. Rev. D **68**, 054006 (2003); A.P. Szczepaniak, Phys. Lett. B **567**, 23 (2003).

[20] A.Hayashigaki and K.Terasaki, Prog. Theor. Phys. **114**, 1191 (2005).